Journal of Radiation Research, 2014, 55, 97–104
doi: 10.1093/jrr/rrt076 Advance Access Publication 31 May 2013

Assessment of anatomical and dosimetric changes by a deformable registration method during the course of intensity-modulated radiotherapy for nasopharyngeal carcinoma

Jie LU[1], Yidong MA[1], Jinhu CHEN[1], Liming WANG[2], Guifang ZHANG[1], Mukun ZHAO[3] and Yong YIN[1,4,*]

[1]Department of Radiation Oncology, Shandong Cancer Hospital and Institute, 440 Jiyan Road, Jinan, 250117, China
[2]Department of Gynaecology, Affiliated Hospital of Medicine School, Qingdao University, 16 Jiangsu Road, Qingdao, 266003, China
[3]Hebei University, 342 Yuhua East Road, 071000, China
[4]Shandong Provincial Key Laboratory of Radiation Oncology, Shandong Academy of Medical Sciences, 440 Jiyan Road, Jinan, 250117, China
*Corresponding author. Department of Radiation Physics, Shandong Cancer Hospital, 440 Jiyan Road, Jinan, 250117, China. Tel: +86-531-6762-6524, Fax: +86-531-6762-6427; Email: yinyongsd@yahoo.com.cn

(Received 23 October 2012; revised 28 April 2013; accepted 28 April 2013)

The aim of this study was to quantify the anatomic variations and the dosimetric effects accessed by a deformable registration method throughout the entire course of radiotherapy, and to evaluate the necessity of replanning for patients with nasopharyngeal carcinoma (NPC). Plan1(CT1) was based on the original CT, and Plan2 (CT2) was generated from the midtreatment CT scan acquired after 25 fractions of IMRT of Plan1. Both sets of CTs, RT structures and RT doses for the two group plans were transferred to a workstation, and then a hybrid IMRT plan, Plan1(CT2), was generated by deforming doses of Plan1 to CT2. Subsequently, the accumulated plan, Plan1 + 2(CT2), was generated to quantify the actual dosimetric effects during the course. The transverse diameter of the neck at the center of the odontoid process was (15.4 ± 1.0) cm and (14.4 ± 1.1) cm in CT1 and CT2, respectively ($P < 0.05$). Compared with CT1, the mean volumes of the right and left parotid glands were significantly decreased by (24.6 ± 11.9)% and (35.1 ± 20.1)%, respectively. Comparison of Plan1 (CT1) with Plan1 (CT2) indicated that the doses to targets decreased without replanning. With repeated CT and replanning after 25 fractions, the doses to targets would be improved. The doses to normal tissue were increased without replanning. For eight patients out of 12, the doses to the spinal cord and brainstem exceeded the constraints without replanning, while the corresponding values decreased with replanning. During the entire course of IMRT, the volumes of the targets and the parotid glands would be reduced significantly. Midtreatment CT scanning and replanning are recommended to ensure adaptive doses to the targets and critical normal tissues.

Keywords: nasopharyngeal carcinoma; deformable registration; dosimetry; radiotherapy plan

INTRODUCTION

Radiotherapy (RT) is a critical component in the current management of patients with nasopharyngeal carcinoma (NPC). Simultaneous integrated-boost intensity-modulated radiation therapy (SIB-IMRT), allowing the simultaneous delivery of different dose levels to different target volumes within a single treatment fraction, has the potential to improve the therapeutic ratio by achieving more conformal dose distribution to the target volumes and better sparing of organs at risk (OARs) [1–3]. Several studies showed that SIB-IMRT improved not only local-regional control, but also quality of life compared with conventional radiation therapy [4–6]. In the setting of SIB-IMRT, due to the sharp dose gradients between the target and normal tissue, even the slightest anatomical changes can result in significant dosimetric changes. The potential dosimetric implications of the anatomical changes may be underdosage of the target

volume and/or overdosage of critical normal tissues [7, 8]. So it is essential to ensure the accurate dose distribution to both targets and normal tissues during the entire course of treatment.

Presently, most IMRT plans are based on a single computed tomography (CT) scan obtained before the start of radiotherapy, which represents only the 'frozen status' at CT scanning. However, it has been demonstrated that many patients with head-and-neck cancer receiving RT develop significant anatomic changes due to weight loss and shrinkage of the primary tumor and/or involved lymph node, especially during the latter part of treatment, and these changes could have potential dosimetric impact when highly conformal treatment techniques are used [9, 10]. Repeated imaging and replanning, even with a single mid-treatment scan, are essential to identify dosimetric changes and to ensure adequate doses to target volumes and safe doses to normal tissues [8, 11]. In our study, an in-house developed program, intensity-based deformable registration algorithm, was used to quantify anatomic changes and actual dosimetric effects with or without replanning for patients with NPC throughout the entire course of the treatment.

MATERIALS AND METHODS

Patient characteristics

A group of 12 patients (median age, 52 years; range, 40–60 years) with locoregionally advanced NPC treated with SIB-IMRT at the Department of Radiation Oncology, Shandong Cancer Hospital between October 2005 and February 2006 were enrolled in this study. Of the 12 patients, nine were male and three were female. Eligible patients were those newly diagnosed with NPC with T3 or T4 and N2 disease according to the 2002 American Joint Committee on Cancer (AJCC) staging classification. The pretreatment evaluations including history and physical examination, nasopharyngoscopy, chest X-ray, complete blood count, liver and renal biochemistry, contrast-enhanced CT and/or magnetic resonance imaging (MRI) of the head-and-neck region were obtained. No patient had known distant metastatic disease. All patients were treated with cisplatin-based concurrent chemotherapy, and underwent repeated CT scanning and replanning after 25 fractions during the course of a total treatment of 30 fractions.

Initial imaging and planning

Patients were immobilized with a head-neck-shoulder thermoplastic mask (CIVCO Medical Solutions, Coralville, IA, USA) in the supine position, and an intravenous contrast-enhanced simulation CT scan was obtained using a slice thickness of 2.5 mm from skull vertex to 3 cm below the clavicles. The initial CT scan (CT1) was performed before treatment and used to generate the original IMRT plan, defined as Plan1(CT1). The simulation CT datasets were transferred to the inverse treatment-planning system (Pinnacle^3 Philips Medical System, Fitchburg, WI, USA), and target volumes and critical normal structures were manually contoured on the axial slices of the planning CT scan by radiation oncologists. The gross target volume (GTV), including nasopharyngeal tumor (GTVnx) and involved lymph nodes (GTVnd), was defined as the tumor visible by either clinical examinations or radiographically with MRI and CT. Clinical target volumes (CTVs), including CTV1 and CTV2 but excluding the GTV, were the regions at high risk for microscopic disease and low risk for elective nodal coverage. CTV1 encompasses the high-risk sites of microscopic extension and the whole nasopharynx; CTV2 encompasses the level of the located lymph node, and the elective neck area (bilateral levels IIa, IIb, III, and Va were routinely covered for all N0 patients, whereas ipsilateral levels IV, Vb, or the supraclavicular fossae were also included for N1 patients). Planning target volumes of the gross target volume (PGTV), PTV1 and PTV2 were defined by three-dimensionally expanding the corresponding target volumes (GTV, CTV1 and CTV2) with a 3-mm margin to compensate for possible residual positional and dosimetric uncertainties. Target prescription doses and critical structures limiting doses were based on the RTOG 0225 trial [12]. The prescribed dose was 66 Gy at 2.2 Gy per fraction to the PGTV, 60 Gy at 2.0 Gy per fraction to the PTV1, and 54 Gy at 1.8 Gy per fraction to the PTV2 for a total of 30 fractions. IMRT plans were calculated by means of a step-and-shoot approach, and the optimization method was performed using Direct Machine Parameter Optimization (DMPO).

Replanning

After 25 fractions of the course of treatment, the second simulation CT scan (CT2) was performed to generate a second IMRT plan, defined as Plan2(CT2), which was used to complete the planned course of treatment. The same patient position was maintained for the two CT scans. Plan1 (CT1) was based on the original CT scan, while Plan2(CT2) was generated from the mid-treatment CT scan (CT2), which was acquired after 25 fractions.

Both sets of CT images, RTstructs and RTdoses were transferred to our deformable registration program, which will be described in the next section. Without cropping or filtering, CT1 and CT2 were first automatically aligned via a global rigid body registration, which can be also adjusted manually according to the region of interest. Second, powered by the Demons deformable registration method, the program deformed CT2 to CT1, and then applied the same CT–CT resultant deformation matrices for co-deforming the RTdose associated with CT1. The deformed dose was named 'Plan1(CT2)'.

Finally the program accumulated the RTdose of Plan1 (CT1) to the RTdose of Plan2(CT2) with the corresponding number of fractions during the process. The resultant

accumulated dose was named 'Plan1 + 2(CT2)', representing the actual situation in which replanning would have occurred.

Deformable registration method

The deformable registration program is based on the Fast Demons (FD) algorithm and its variants are widely used in fast deformable 3D registration. The original algorithm of Demons is based on the optical flow [13]. In the Demons variant study, the displacement of each voxel is mostly given by:

$$\vec{d} = -\frac{(f-m)\vec{\nabla}f}{||\vec{\nabla}f||^2 + (f-m)^2/K} \quad (1)$$

where f and $\bar{\nabla}f$ is the voxel intensity and the gradient of the fixed volume (CT1), m is the intensity of the point in the moving volume (CT2), and k is the normalization factor. We can improve (1) for better preform by considering the gradient of both volumes [14]:

$$\vec{d} = -\frac{(f-m)(\vec{\nabla}f + \vec{\nabla}m)}{||\vec{\nabla}f + \vec{\nabla}m||^2 + (f-m)^2/K} \quad (2)$$

Now the gradient of the deformed moving volume ($\bar{\nabla}m$) is included. Unfortunately, the speed may be slower than the original algorithm due to the calculating the gradient of the moving volume. Because our plan was calculated off-line, prolonged computation time is not so critical.

Volume comparisons

The volumes of the PGTV, PTV1, PTV2 and the bilateral parotid were compared between the first and second CT scans. In this analysis, the OARs include spinal cord, brainstem, eyes, lenses, optic nerves and parotid glands. In addition, the odontoid process was contoured on every CT scan and the center point was calculated by computer as a reference to quantify the anatomic changes. At the center of the odontoid process, the transverse diameter of neck was measured and compared.

Dosimetric comparisons

Dose–volume histograms (DVHs) of the targets and OARs from Plan1(CT1), Plan1(CT2) and Plan1 + 2(CT2) were analyzed. Plan1(CT1) was compared with Plan1(CT2) to investigate the effect of anatomic changes on dosimetric outcomes, and Plan1(CT2) and Plan1 + 2(CT2) were compared to investigate the effect and the necessity of replanning. The dosimetric parameters [including the dose to 95% of the target (D_{95}), the mean dose to the target (D_{mean}), the maximum dose (D_{max}) and the dose to 1cm^3 ($D_{1\ cm^3}$) of the spinal cord and brainstem, eyes, optic nerves, and lenses, and the percent of the volume of the parotid glands receiving ≥30 Gy (V_{30})] were compared.

Statistical analysis

Descriptive statistics were calculated to characterize the dose and volume for targets and OARs. Comparison between the paired CT volume measurements and dosimetric parameters of the original, hybrid and accumulated IMRT plans were analyzed using the non-parametric Wilcox signed rank test. All statistical tests were two-sided, with a threshold for statistical significance of a P-value < 0.05. Statistical analyses were carried out using SPSS version 17.0 software.

RESULTS

Volumetric changes in targets and normal tissues

Figure 1 illustrates the measurement of the transverse diameter at the center of the odontoid process. The transverse diameter of the neck at the center of the odontoid process was (15.4 ± 1.0) cm and (14.4 ± 1.1) cm in CT1 and CT2, respectively ($P < 0.05$). The volume comparison of targets and parotid glands in the first and second CT scans were reported in Table 1, and an example of the volumetric changes was shown in Fig. 2. There was no significant difference in the volume of the PGTV, PTV1 and PTV2 between the first and second CT scans. However, compared with CT1, the median volume reduction of the right and left parotid glands was 4.9 cm^3 and 7 cm^3, respectively, or a decrease of (24.6 ± 11.9)% and (35.1 ± 20.1)% of the initial volume in CT2 with a significant difference of ($P < 0.05$).

Dosimetric comparisons

The dosimetric difference between replanning and not replanning of targets and OARs is illustrated in Tables 2 and 3, and a representative dose distribution comparison of

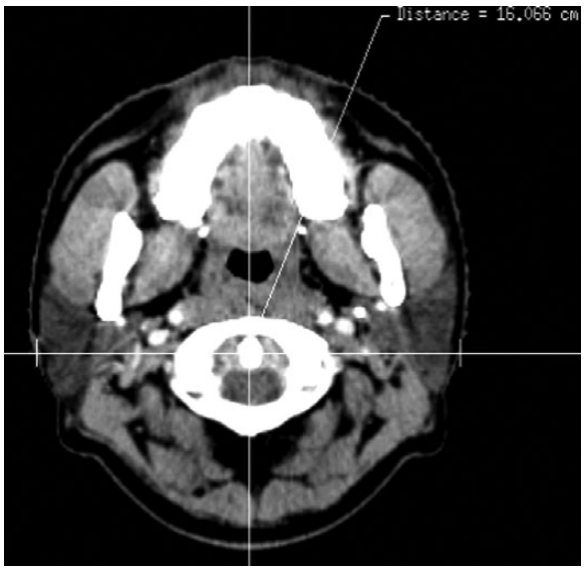

Fig. 1. Measurement of transverse diameter at the center of odontoid process.

Table 1. Volume comparison between CT scans (cm^3, $\bar{x} \pm S$)

Target	CT1	CT2	Mean % change	*P*
PGTV	240.5 ± 91.3	196.9 ± 86.7	−16.4 ± 27.3	0.128
PTV1	520.5 ± 99.8	538.1 ± 98.9	3.8 ± 6.3	0.237
PTV2	370.4 ± 51.2	338.6 ± 65.5	−8.8 ± 12.0	0.237
Parotid (right)	18.6 ± 10.8	13.5 ± 7.3	−24.6 ± 11.9	0.018
Parotid (left)	19.7 ± 9.8	12.7 ± 7.9	−35.1 ± 20.1	0.018

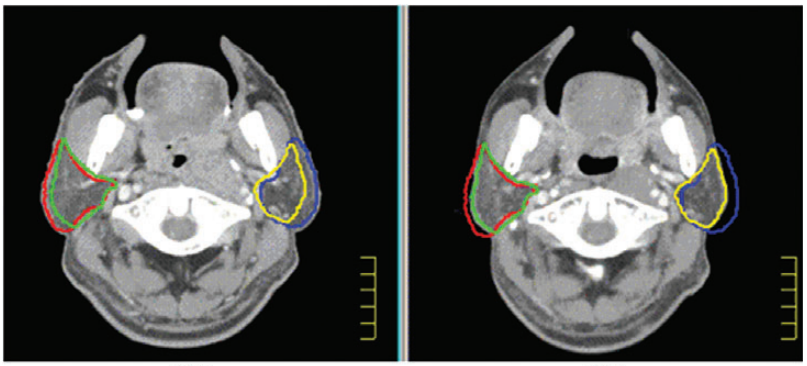

Fig. 2. An example of the volumetric changes for the parotid glands between the first CT (CT1) and the second CT (CT2) images. Shown on images are right parotid contour (red) and left parotid contour (blue) for CT1, and right parotid contour (green) and left parotid contour (yellow) for CT2.

Table 2. Summary of dosimetric results for PTV(Gy, $\bar{x} \pm S$)

Target	Parameter	Plan1(CT1)	Plan1(CT2)	Plan1 + 2 (CT2)
PGTV	D_{mean}	69.4 ± 0.7	68.6 ± 0.4[a]	68.9 ± 0.5[b]
	D_{95}	66.5 ± 0.8	63.9 ± 1.3[a]	65.4 ± 1.0[b]
PTV1	D_{mean}	63.6 ± 0.9	63.7 ± 1.1	63.8 ± 1.0
	D_{95}	59.6 ± 1.3	56.3 ± 1.7[a]	58.0 ± 1.3[b]
PTV2	D_{mean}	57.1 ± 1.0	55.3 ± 1.7[a]	56.0 ± 1.0[b]
	D_{95}	54.5 ± 0.9	37.2 ± 23.1[a]	46.6 ± 9.7[b]

*Statistical significance with $P < 0.05$. [a]Plan1(CT2) vs Plan1 (CT1); [b]Plan1 + 2(CT2) vs Plan1(CT2).

treatment planning during the course of IMRT is shown in Fig. 3. The data demonstrate that without repeated imaging and replanning during the course of IMRT, the doses to targets were reduced and the doses to critical normal tissues were increased.

Target volumes

Compared with Plan1(CT1), D_{95} to the PGTV, PTV1 and PTV2, and D_{mean} to the PGTV and PTV2 decreased significantly in Plan1(CT2), which indicate the doses to targets decreased without replanning. With repeated CT and replanning after 25 fractions as shown in Plan1 + 2(CT2), the doses to targets would be improved. The dosimetric difference with replanning could be smaller, so replanning is necessary to ensure adequate dose to targets.

Organs at risk

Comparing Plan1(CT2) with Plan1(CT1), D_{max} and $D_{1\ cm^3}$ of the spinal cord and brainstem increased without replanning, although no statistical significance was observed. The difference between replanning and not replanning could be greater. In eight patients out of 12, the doses to the spinal cord and brainstem exceeded the constraints without replanning, while the corresponding values decreased with replanning. Simultaneously, the same trend was observed in the parotid glands. Without replanning D_{mean} and V_{30} to the parotid glands increased, although these changes were not statistically significant, but with replanning the doses to the parotid glands were decreased.

DISCUSSION

IMRT has become a major treatment modality for NPC patients, and requires high precision in treatment delivery and patient positioning. The steep dose gradients of IMRT require accurate patient positioning because small variations in setup may cause significant shifts of dose [15–17]. Many

Table 3 Summary of dosimetric results for OARs ($\bar{x} \pm S$)

OARS	Parameter	Plan1(CT1)	Plan1(CT2)	Plan1 + 2(CT2)
Spinal cord	D_{max}(Gy)	41.9 ± 0.8	43.5 ± 2.9	42.1 ± 1.1
	D_{1cc}(Gy)	39.6 ± 1.1	40.7 ± 2.4	40.3 ± 1.6
Brainstem	D_{max}(Gy)	57.9 ± 1.7	58.4 ± 3.4	57.2 ± 2.7
	D_5(Gy)	48.8 ± 3.4	49.5 ± 3.1	49.3 ± 2.7
Right parotid	D_{mean}(Gy)	32.6 ± 3.8	32.4 ± 1.9	32.0 ± 2.4
	V_{30}(%)	47.7 ± 10.6	48.5 ± 6.6	46.7 ± 6.4
Left parotid	D_{mean}(Gy)	32.7 ± 2.3	33.9 ± 5.9	33.1 ± 3.8
	V_{30}(%)	48.1 ± 6.7	51.0 ± 20.6	48.9 ± 13.9
Right eye	D_{max}(Gy)	21.1 ± 10.2	21.0 ± 8.3	21.8 ± 6.3
Left eye	D_{max}(Gy)	20.1 ± 9.9	21.5 ± 8.3	22.2 ± 5.6
Right optic nerve	D_{max}(Gy)	42.3 ± 13.5	45.5 ± 13.2	44.1 ± 12.4
Left optic nerve	D_{max}(Gy)	40.1 ± 15.0	39.8 ± 12.0	36.9 ± 12.8
Right lens	D_{max}(Gy)	6.0 ± 1.0	5.8 ± 1.1	5.8 ± 0.9
Left lens	D_{max}(Gy)	6.0 ± 1.0	5.8 ± 1.2	5.9 ± 1.0

*Statistical significance with $P > 0.05$.

institutions are currently using cone beam CT (CBCT) or other advanced technologies to decrease the impact of setup error. However, without replanning, its use is inadequate to address the dosimetric effects related to changes in the internal target and normal organs [18]. Patients may have significant anatomic changes during the course of radiation therapy because of shrinkage of the primary tumor and/or involved lymph nodes, and weight loss because of poor oral intake [7, 9]. Such magnitude of volumetric and positional changes has significant effects on dose distribution.

In the process of IMRT in NPC patients, Barker *et al.* [9] reported that the changes in the targets and normal organs appeared to be significant during the second half of treatment (after 3–4 weeks of treatment) and could have a potential dosimetric impact when highly conformal treatment techniques are used. Recent studies demonstrated the importance of repeated CT planning during the course of IMRT for locoregionally advanced NPC [8, 19–21]. In our study, the second simulation CT scan (CT2) was performed to generate a second IMRT plan after 25 fractions of the course of treatment, and the deviation between the planned and delivered dose of IMRT from the original plan was measured based on an intensity-based deformable registration algorithm. It should be noted that, due to time and cost, only one repeated CT was scanned for each case. Anatomic changes had occurred and would continue, even though the rescanning was arranged after 25 fractions. In the study, we intended to demonstrate the anatomic changes and the consequent dose changes, and to point out the importance of adjustment and replanning. In our previous study (unpublished), in order to eliminate setup errors between the two CT scans, the spatial relationship between the isocenters of the two CT scans was established by using CT–CT fusion based on bony landmarks. For the deformed plans, the first IMRT plan was applied to the second CT scan according to the spatial relationship of the isocenters of the two CT scans, as determined by CT–CT fusion. In our investigation, deformable registration was used for not only image registration but also for determining deformable dose accumulation by different structures of the patient's anatomy, accurately considering anatomy changes and position differences of the target and OARs between the initial and the repeated simulation CTs during the course of the radiotherapy. Initiation of a new plan provides more intuitive evaluation of dose change and dose accumulation of patients. It needs to be made clear that the dose accumulation, or so-called 'dose mapping' used in deformable registration in this study, was not equal to actual dose distribution. The dose map was deformable transformed to another CT image by voxel to voxel. Recently, several groups have compared dose deformation using experimental methods with that using deformable registration algorithms [22, 23]. Neither of the two approaches can exactly represent the actual dose build-up and distribution, due to electron lateral scattering and equilibrium when the irradiation volume and pathway are changed. Therefore, one should be aware of the potential pitfalls in evaluating a treatment course using dose deformable registration algorithms.

There exist a number of deformable registration algorithms, and their variants being widely used in both clinical and experimental applications. In a recent study, Kirby *et al.* [24] compared 11 algorithms, including the FD algorithm, in

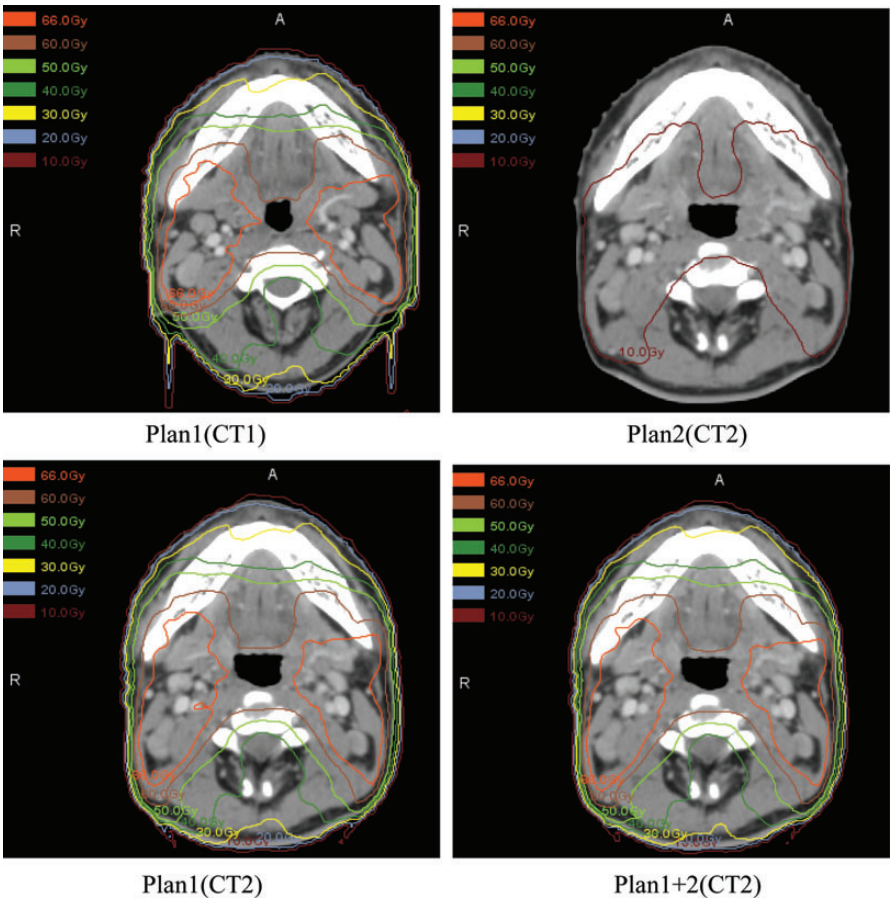

Fig. 3. The dose distribution comparison of treatment planning during the course of IMRT. Plan 1(CT1) is the original plan based on the first CT scan; Plan2 (CT2) is the second IMRT with only the number of fractions used to complete the treatment based on the second CT; Plan1(CT2) is first IMRT plan deformed to the second CT scan; Plan1 + 2(CT2), representing the actual situation in which replanning would have occurred, is the accumulation of Plan1(CT1) and Plan2(CT2).

a deformable phantom to evaluate the transformation accuracy, with a Dice similarity coefficient. The values of the coefficient for the FD, Fast iterative Optical Flow (FOF), and Fast Demons with Elastic regularization (FDE) algorithm were 0.93, 0.94 and 0.93, respectively. (The best evaluation value is 1.0.) These were higher than when using other algorithms. Wang *et al.* [25], setting a mathematical transformation for a number of head-and-neck CTs as the ground truth, investigated the accuracy of the Demons algorithm, showing that > 96% of voxels presented shifting errors within 2 mm. The FD algorithm was also applied to the deformable registration of the dose maps, although it was not considered to be as accurate as when applied to CT images [24].

One belief was that the original plan treatment beam could copy to the second CT. In that way, the dose map could better represent the actual distribution. Yet that is the way we operated daily for each patient over the treatment course. The application of deformable registration in this study was to demonstrate the program and its clinical feasibility. Furthermore, in favor of deformable registration, anatomic changes and dose changes can be viewed more directly, even though a calculation rather than actual reality is being represented.

Our results showed that the mean volume of the right and left parotid glands decreased between the original CT and the second CT scans ($P = 0.018$, $P = 0.018$, respectively). There were no significant differences in the volumes of other contoured normal structures or target volumes seen between the two CT scans. However, when comparing the dosimetric effects of replanning vs not replanning, the Plan1(CT2) demonstrated both decreased doses to target volumes and increased doses to normal structures. Comparison of Plan1 + 2(CT2) and Plan1(CT2) showed that if the patient's radiotherapy treatment plan was modified in a timely way, the accumulated dose was closer to the requirements of the prescription dose. If we do not modify the treatment plan during a course of therapy, the dose to the targets will be decreased and the dose to the OARs will be increased due to the volumetric changes in the target and OARs; if we modify

the plan in a timely fashion, the cumulative dose to some OARs will be reduced. For NPC patients, the maximum point dose to the spinal cord and brain stem is very important in the evaluation of OAR dose parameters. Although there were no statistically significant differences for the maximum dose to the brainstem and spinal cord between replanning and not replanning, eight of the 12 patients were out of constraint criteria in our hospital. If we remodified the plan, the cumulative dose in actual therapy would meet the clinical requirements.

CONCLUSION

For NPC patients receiving IMRT, the volume of the target and parotids clearly decreased during therapy, the doses to target volumes decreased, and the doses to the parotid glands, spinal cord and brainstem were increased. Our results show that repeated CT imaging and replanning during the course of IMRT is essential for identifying dosimetric changes and to ensure adequate doses to target volumes and safe doses to normal tissues. We plan to undertake further studies to validate this conclusion for two or more CT scans, and also to investigate the off-line correction technology of CBCT for observing changes in tumor target, parotid glands and other tissues.

FUNDING

This work was supported by grants from the Shandong Natural Science Fund [ZR2009CL032] and the National Natural Science Fund [61201441].

ACKNOWLEDGEMENTS

The authors would like to thank their colleagues for their support in data collection.

REFERENCES

1. Chen S-W, Yang S-N, Liang J-A *et al*. Comparative dosimetric study of two strategies of intensity-modulated radiotherapy in nasopharyngeal cancer. *Med Dosim* 2005;**30**:219–27.
2. Chung J-B, Lee J-W, Kim J-S *et al*. Comparison of target coverage and dose to organs at risk between simultaneous integrated-boost whole-field intensity-modulated radiation therapy and junctioned intensity-modulated radiation therapy with a conventional radiotherapy field in treatment of nasopharyngeal carcinoma. *Radiol Phys Technol* 2011;**4**:180–4.
3. Kam M, Chau R, Suen J *et al*. Intensity-modulated radiotherapy in nasopharyngeal carcinoma: dosimetric advantage over conventional plans and feasibility of dose escalation. *Int J Radiat Oncol Biol Phys* 2003;**56**:145–57.
4. Martin E, Deville C, Bonnetain F *et al*. Intensity-modulated radiation therapy in head and neck cancer: prescribed dose, clinical challenges and results. *Radiother Oncol* 2007;**85**:392–8.
5. Wong F-C, Ng A-W, Lee V-H *et al*. Whole-field simultaneous integrated-boost intensity-modulated radiotherapy for patients with nasopharyngeal carcinoma. *Int J Radiat Oncol Biol Phys* 2010;**76**:138–45.
6. Xiao W-W, Huang S-M, Han F *et al*. Local control, survival, and late toxicities of locally advanced nasopharyngeal carcinoma treated by simultaneous modulated accelerated radiotherapy combined with cisplatin concurrent chemotherapy: long-term results of a phase 2 study. *Cancer* 2011;**117**:1874–83.
7. Bhide S-A, Davies M, Burke K *et al*. Weekly volume and dosimetric changes during chemoradiotherapy with intensity-modulated radiation therapy for head and neck cancer: a prospective observational study. *Int J Radiat Oncol Biol Phys* 2010;**76**:1360–8.
8. Hansen E-K, Bucci M-K, Quivey J-M *et al*. Repeat CT imaging and replanning during the course of IMRT for head-and-neck cancer. *Int J Radiat Oncol Biol Phys* 2006;**64**:355–62.
9. Barker J-L, Garden A-S, Ang K-K *et al*. Quantification of volumetric and geometric changes occurring during fractionated radiotherapy for head-and-neck cancer using an integrated CT/linear accelerator system. *Int J Radiat Oncol Biol Phys* 2004;**59**:960–70.
10. Vasquez Osorio E-M, Hoogeman M-S, Al-Mamgani A *et al*. Local anatomic changes in parotid and submandibular glands during radiotherapy for oropharynx cancer and correlation with dose, studied in detail with nonrigid registration. *Int J Radiat Oncol Biol Phys* 2008;**70**:875–82.
11. Han C, Chen Y-J, Liu A *et al*. Actual dose variation of parotid glands and spinal cord for nasopharyngeal cancer patients during radiotherapy. *Int J Radiat Oncol Biol Phys* 2008;**70**:1256–62.
12. RTOG Protocol 0225: A phase II study of IMRT +/- chemotherapy for nasopharyngeal cancer. http:// www.rtog.org (15 December 2006, date last accessed).
13. Thirion J-P. Image matching as a diffusion process: an analogy with Maxwell's demons. *Med Image Anal* 1998;**2**:243–60.
14. Nithiananthan S, Brock K-K, Irish J-C *et al*. Deformable registration for intra-operative cone-beam CT guidance of head and neck surgery. *Conf Proc IEEE Eng Med Biol Soc* 2008;**2**:3634–7.
15. Astreinidou E, Bel A, Raaijmakers C-P *et al*. Adequate margins for random setup uncertainties in head-and-neck IMRT. *Int J Radiat Oncol Biol Phys* 2005;**61**:938–44.
16. Siebers J-V, Keall P-J, Wu Q *et al*. Effect of patient setup errors on simultaneously integrated boost head and neck IMRT treatment plans. *Int J Radiat Oncol Biol Phys* 2005;**63**:422–33.
17. Zhang L, Garden A-S, Lo J *et al*. Multiple regions-of-interest analysis of setup uncertainties for head-and-neck cancer radiotherapy. *Int J Radiat Oncol Biol Phys* 2006;**64**:1559–69.
18. Wang J, Bai S, Chen N *et al*. The clinical feasibility and effect of online cone beam computer tomography-guided intensity-

modulated radiotherapy for nasopharyngeal cancer. *Radiother Oncol* 2009;**90**:221–7.
19. Wang W, Yang H, Hu W *et al*. Clinical study of the necessity of replanning after the 25th fraction during the course of intensity-modulated radiotherapy for patients with nasopharyngeal carclinoma. *Int J Radiat Oncol Biol Phys* 2010;**77**:617–21.
20. Wang X, Lu J, Xiong X *et al*. Anatomic and dosimetric changes during the treatment course of intensity-modulated radiotherapy for locally advanced nasopharyngeal carcinoma. *Med Dosim* 2010;**35**:151–7.
21. Wu Q, Chi Y-W, Chen P-Y *et al*. Adaptive replanning strategies accounting for shringkage in head and neck IMRT. *Int J Radiat Oncol Biol Phys* 2009;**75**:924–32.
22. Niu C-J, Foltz W-D, Velec M *et al*. A novel technique to enable experimental validation of deformable dose accumulation. *Med Phys* 2012;**39**:765–76.
23. Yeo U-J, Taylor M-L, Dunn L *et al*. A novel methodology for 3D deformable dosimetry. *Med Phys* 2012;**39**: 2203–13.
24. Kirby N, Chuang C, Ueda U *et al*. The need for application-based adaptation of deformable image registration. *Med Phys* 2013;**40**:011702.
25. Wang H, Dong L, O'Daniel J *et al*. Validation of an accelerated 'demons' algorithm for deformable image registration in radiation therapy. *Phys Med Biol* 2005;**50**: 2887–905.